Sādhanā (2021)46:25
https://doi.org/10.1007/s12046-020-01542-8

Onset of natural convection in a differentially heated layer of gray and non-gray gas mixtures

SHASHIKANT CHOLAKE[1], T SUNDARARAJAN[1,*] and S P VENKATESHAN[2]

[1]Department of Mechanical Engineering, Indian Institute of Technology Madras, Chennai, India
[2]Department of Mechanical Engineering, IIIT Design and Manufacturing Kancheepuram, Chennai, India
e-mail: tsundar@iitm.ac.in

MS received 4 March 2020; revised 15 October 2020; accepted 6 November 2020

Abstract. The onset of convection instability in a differentially heated layer consisting of gray and non-gray gaseous mixtures is studied numerically. The conditions investigated cover a wide range of Planck number values ($Pl = \frac{\kappa k_T}{4\sigma T_0^3}$), from the conduction-dominated regime of $Pl \gg 1$ to the radiation-dominated regime of $Pl \ll 1$. The linear stability theory is applied to mass, momentum and energy balance equations and the resulting linear stability equations are solved by Chebyshev spectral collocation method. The divergence of radiative flux is solved by the finite-volume-based discrete ordinates method. The Spectral Line Weighted sum of gray gas (SLW) model is used to represent the fine spectral variation of absorption coefficient for a non-gray gas medium. The results indicate that the critical Rayleigh number (Ra_c) for the onset of convection increases with mean temperature (T_0) in the conduction-dominated regime at low values of T_0. In the radiation-dominated regime ($Pl \ll 1$), Ra_c decreases with T_0 for gray media. If the medium is non-gray, the critical Ra_c reduces to even lower values (as compared with those of gray gases) due to the dependence of gas absorptivity on temperature T_0. A reduction in the wall emissivity value increases the stability of the fluid layer due to reflection of radiation from the wall, in the radiation-dominated regime. The reverse trend is seen for $Pl \gg 1$. The critical parameters also significantly depend on the concentrations of radiatively participating gases in the mixture. The temperature profile in the fluid layer transforms from a linear profile in conduction regime to a stratified profile with steep gradients near the walls, in the presence of non-gray participating gases.

Keywords. Onset of convection; gray and non-gray gas mixtures; Planck number; stability.

1. Introduction

Natural convection flows are driven by density gradients prevailing across a fluid medium. In differentially heated fluid layers for which heat is supplied at the bottom wall, onset of convection takes place only if the buoyancy force due to density gradient is able to overcome the viscous resistance of the fluid. This is characterized by the Rayleigh number (Ra) exceeding a critical value, for the heat transfer process to change from pure conduction mode to convective-diffusion mode. In the presence of participating gas layers, radiation heat transfer also has significant effect depending on the gas species involved, average temperature of the medium and wall emissivity values. Several authors have addressed the onset of convection in a fluid layer by various solution methodologies [1–3] and reported their results in terms of critical Rayleigh number (Ra_c) and wave number (k_c) values. If the medium consists of a fluid such as carbon dioxide or water vapor which actively participates in radiative heat transfer, the volumetric radiation heat flux significantly alters the initial temperature distribution and fluid flow patterns within the medium after the onset of convection. Such cases can be observed in solar collectors, heat exchangers, furnaces, atmospheric processes, geophysical and astrophysical applications, to name a few. In particular, during fire break-out scenarios in enclosures, combustion products such as carbon dioxide and water vapor can alter the radiative properties of the gaseous medium significantly and thereby modify the evolution of natural convective flow and heat transfer. Understanding the onset of natural convective instability in a radiatively active fluid layer can be the first step to develop the methodology for solving such complex problems. Additionally, it is important to obtain a good insight into the effects of mixture composition, mean gas temperature and the enclosure wall conditions on the resulting temperature profiles as well as the multi-mode heat transfer phenomena.

*For correspondence
Published online: 04 February 2021

With regard to multi-mode heat transfer, Gille and Goody [4] studied theoretically and experimentally the onset of convection in dry air and ammonia, with ammonia serving as a radiating fluid. The experimental results were found to be in good agreement with theoretical predictions. Spiegel [5], by variational principle, obtained the critical Rayleigh number values for a wide range of medium optical thickness values, with rigid bounding surfaces. Christophorides and Davis [6] incorporated the initial nonlinear temperature profile for radiating fluid medium to obtain the critical parameters for the onset of convection. The effects of non-gray radiating fluid on critical Rayleigh number and wave number were studied by Arpaci and Gózúm [7] in terms of the Planck and Rosseland mean absorption coefficients. Lienhard [8] reports a strong dependence of fluid layer stability on thermal radiation from finite conducting boundaries, which has implication in solar collector design. A parametric study has been carried out by Bdéoui and Soufiani [9] in the presence of molecular radiating gases such as CO_2 and H_2O. It is found that the optical thickness, wall emissivity and static temperature profile have strong influence on the onset of flow instability.

Hutchson and Richards [10] studied the thermal instability of a horizontal fluid layer of air and CO_2. They reported that the non-grayness of carbon dioxide and initial temperature distribution play an important role in the layer stability. Bifurcation sequence for Rayleigh–Bénard convection in small enclosures was studied by Mukutmoni and Yang [11]. Lan *et al* [12] studied the stability of Rayleigh–Bénard convection in a three-dimensional domain using the spectral method. They showed that the non-linear static temperature profile due to volumetric radiation influences the critical parameters significantly. The authors also highlighted the effects of conduction–radiation parameter, Rayleigh number and optical thickness. Yang [13], using linear stability theory, studied the effects of Planck number, optical thickness, Biot number and wall emissivity on convection instability. The radiation-induced convection in nocturnal atmospheric conditions was studied analytically and experimentally by Prasanna and Venkateshan [14]. A similar study for dry atmospheric convective instability was carried out by Larson[15] considering the effect of thermal diffusivity on static temperature distribution and critical threshold values, i.e., Rayleigh number. Moufekkir *et al* [16] numerically studied the fluid stratification phenomena in a differentially heated square cavity due to variation of Planck number.

Aforementioned works on Rayleigh–Benard instability in a radiatively participating fluid primarily considered gray participating media with different boundary conditions and solution techniques. The changes in the fluid layer stability with mean temperature (T_0), starting from the conduction-dominated regime (low T_0 or $Pl \to \infty$) to radiation-dominated regime (high T_0 or $Pl \to 0$), have not been addressed comprehensively in the available works. Because of shift in the main mode of heat transfer (conduction to radiation), the resulting temperature profile within the fluid layer and the onset of convective instability undergo drastic changes. Furthermore, non-gray absorption behavior of the fluid layer significantly modifies the critical parameters for convective instability. Therefore, the mixture composition and wall boundary conditions also influence the fluid layer instability.

The main objective of the present study is to develop a numerical solution procedure to simulate the onset of natural convection in an infinite horizontal layer of gray/non-gray gases. The spectral technique based on Chebyshev polynomial expansion is employed for analyzing the linear stability behavior of the fluid medium.

A mixture of gray and non-gray participating media bounded by differentially heated rigid walls is considered. The actual spectral absorption coefficient variation is modeled by the Spectral Line Weighted sum of gray gas (SLW) approach for non-gray gases such as carbon dioxide and water vapor. Detailed parametric studies involving variations in the mean operating temperature, composition of gas mixture and wall emissivity are carried out. In particular, changes that occur in the fluid layer stability over a wide range of conditions starting from conduction-dominated situations ($Pl \gg 1$) to radiation-dominated cases ($Pl \ll 1$) are highlighted in detail.

2. Basic equations and formulation

The physical domain consists of an infinite horizontal fluid layer of a gray or non-gray gas mixture, confined between bottom and top walls, which are maintained at the uniform temperatures of $T_1 = T_0 + 0.5\Delta T$ and $T_2 = T_0 - 0.5\Delta T$ respectively. The walls are separated by distance 'd' (figure 1) and the density variation is represented in terms of the Boussinesq approximation with an appropriate choice of ΔT. The thermophysical properties of the gas mixture are calculated at the mean temperature (T_0), following the work of Dandy [17]. The governing equations for mass, momentum and energy are

$$\nabla \cdot \vec{V} = 0 \tag{1}$$

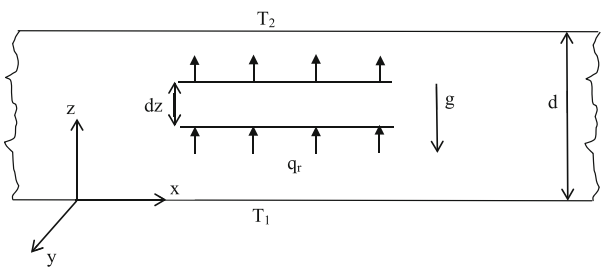

Figure 1. Schematic of physical domain.

$$\frac{\partial \vec{V}}{\partial t} + \vec{V} \cdot \nabla \vec{V} = -\frac{\nabla P}{\rho} + \vec{g}\beta(T - T_0) + \nu \nabla^2 \vec{V} \tag{2}$$

$$\frac{\partial T}{\partial t} + \vec{V} \cdot \nabla T = \frac{k_T}{\rho C_p} \nabla^2 T - \frac{1}{\rho C_p} \nabla \cdot q_r \tag{3}$$

where $\nabla \cdot q_r$ is the volumetric radiative source term. Linear stability theory is applied to analyze the system evolution after the introduction of infinitesimal disturbances in the basic steady state solution. One can obtain the basic steady state (quiescent fluid) solution by setting $\vec{V} = 0$ and the resulting equations are

$$\nabla P = \rho \vec{g} \beta (T - T_0) \tag{4}$$

$$k_T \frac{d^2 T}{dz^2}\bigg|_s = \frac{dq_r}{dz}\bigg|_s \tag{5}$$

For a differentially heated horizontal layer, Eq. (5) represents the energy flux balance in the vertical direction (figure 1) where q_r denotes the radiation energy flux arriving from or leaving to all directions in an integrated hemispherical sense. The two limiting solutions of Eq. (5) correspond to the conduction solution for a radiatively non-participating medium ($q_r \to 0$) and the radiation-dominated regime for a participating medium with thermal conductivity $k_T \to 0$; these solutions can be analyzed in terms of the Planck number ($Pl = \frac{\kappa k_T}{4\sigma T_0^3}$) as cases corresponding to $Pl \to \infty$ and $Pl \to 0$, respectively. Interesting changes in the temperature profile and critical parameters for the onset of convective instability are predicted for Pl variation from 0 to ∞. For linear stability analysis, infinitesimal perturbations of the basic solution are defined by the fields

$$\vec{V}^* = 0 + \vec{v}, \tag{6}$$

$$T^* = T_s + \theta_p, \tag{7}$$

$$q_r^* = q_{r,s} + q_r. \tag{8}$$

In Eqs. (7) and (8), T_s and $q_{r,s}$ are the static temperature field and the corresponding divergence of radiative flux, respectively, satisfying Eq. (5). Incorporating the perturbed field expansions of Eqs. (6)–(8) into Eqs. (1)–(3) and taking the double curl of momentum equation results in linearized equations for the perturbed fields. A normal mode analysis is applied to the linearized equations by expressing the disturbance fields as [18]

$$w = W(Z) exp\left[i\left(k_x x + k_y y\right) + \sigma t\right], \tag{9}$$

$$\theta_p = \phi(Z) exp\left[i\left(k_x x + k_y y\right) + \sigma t\right], \tag{10}$$

$$\nabla \cdot q_r = Q(Z) exp\left[i\left(k_x x + k_y y\right) + \sigma t\right]. \tag{11}$$

Here k_x, k_y are the wave numbers of the disturbances in the x and y directions (of infinite extent), σ is the growth rate of disturbance and $\nabla \cdot q_r$ is the perturbed radiative flux divergence, which depends linearly on $Q(Z)$. Also, w and θ_p are the perturbed dimensionless vertical velocity and temperature fields, respectively. Letting $D = \frac{d}{dz}$ and $k^2 = k_x^2 + k_y^2$, the resulting linear equations are

$$D^4 W - \left(2k^2 + \sigma\right) D^2 W + \left(k^4 + k^2 \sigma\right) W = \frac{Ra}{Pr} k^2 \phi \tag{12}$$

$$D^2 \phi - k^2 \phi - Pr\sigma\phi = Pr\alpha_s W + B_0 Q \tag{13}$$

where Ra is the Rayleigh number $\left(Ra = \frac{g\beta\Delta T d^3}{\nu\alpha}\right)$, Pr is the Prandtl number $\left(Pr = \frac{\nu}{\alpha}\right)$ and α_s is the dimensionless static temperature gradient. The quantity $B_0\left(= \frac{d^2}{\rho C_p \nu \Delta T}\right)$, when multiplied with $\nabla \cdot q_r$, results in the dimensionless source term. With no-slip condition prescribed on the walls, the velocity and temperature disturbances vanish at the boundaries; thus, the boundary conditions are

$$DW = 0, W = \phi = 0 \tag{14}$$

at $Z = 0, 1$.

The spectral collocation method is adapted to solve the perturbation equations (Eqs. 12 and 13) with boundary conditions (Eq. 14), to analyze the convective stability of the horizontal layer consisting of radiatively participating gases. The amplitudes of disturbance functions $W(Z)$ and $\phi(Z)$ are expressed as series expansions in terms of basis functions over N Chebyshev collocation points [19, 20]. The resulting stability equations reduce to a linear eigenvalue problem of the form

$$AX = \sigma BX \tag{15}$$

where A and B are known matrices of size $2N \times 2N$ and X is an unknown vector containing the expansion coefficients. The eigen-system (Eq. 15) has $2N$ eigenvalues and eigenvectors. The stability of the system for a given wave number (k) of the disturbance field is found by searching for eigenvalues with negative, zero and positive real part. For a stable system, all eigenvalues should have negative real part; even if one of the eigenvalues is positive the system is unstable. A marginally stable condition separates stable and unstable domains of operation and it is characterized by an eigenvalue with zero real part.

3. Numerical evaluation of divergence of radiative flux with SLW model for a non-gray gas

The divergence of radiative flux $\nabla \cdot q_r$ is evaluated numerically by solving the Radiative Transfer Equation (RTE) by finite-volume-based discrete ordinates method [21]. The non-gray absorption coefficient is represented by the SLW model [22, 23]. RTE, after incorporating the SLW model, is written as

$$\frac{\partial I_j}{\partial s} = \kappa_j a_j I_b - \kappa_j I_j \tag{16}$$

where j is the gray gas index and κ_j, a_j are, respectively, the absorption coefficient and the corresponding black body weight function; they are evaluated by following the work of Pearson *et al* [23]. In the present study, the absorption behavior of non-gray gases like CO_2 and H_2O is represented as equivalent to the weighted absorption behavior of 'm' gray gases. The RTE is solved for each gray gas and the total intensity is the sum of intensity of each gray gas, $I = \sum_{j=1}^{m} I_j$, where 'm' is the number of gray gases (the value of $m = 20$ is chosen for the present simulations).

The intensity at the boundary is

$$I_w = \epsilon_w a_j I_b(T_w) + \frac{1-\epsilon_w}{\pi} \int I |\vec{n} \cdot \vec{s}| d\Omega \tag{17}$$

where $\vec{n}$ and $\vec{s}$ are, respectively, the unit surface normal and directional vectors. Also, Ω is the solid angle. In the numerical simulations, contributions from 48 directions are considered to evaluate the integral on the right hand side of Eq. (17). The perturbation in temperature (θ_p) modifies the intensity field through the absorption coefficients and the corresponding black body weights (κ_j and a_j) and the black body intensity (I_b). Expanding the temperature and intensity fields in terms of a steady part (T_s and $I_j(T_s)$) and a perturbation part (θ_p and I_j') for each gray gas, the RTE is rewritten as

$$\frac{\partial I_j'}{\partial s} = \kappa_j a_j (T_s) \frac{\partial I_b}{\partial T}\bigg|_{T_s} \theta_p + \frac{\partial \kappa_j a_j}{\partial T}\bigg|_{T_s} I_b(T_s)\theta_p - \kappa_j I_j'. \tag{18}$$

The corresponding perturbed intensity at the wall becomes

$$I_w' = \frac{1-\epsilon_w}{\pi} \int I' |\vec{n} \cdot \vec{s}| d\Omega. \tag{19}$$

Solving the RTE (Eq. 18) for the perturbed intensity field and summing the divergence of radiative flux for each gray gas over 4π solid angle leads to the evaluation of the disturbed radiative flux divergence in the form

$$\nabla \cdot q_r = Q(Z) exp\left[i\left(k_x x + k_y y\right) + \sigma t\right] \tag{20}$$

where $Q(Z)$ is the total radiative disturbance, evaluated as

$$Q(Z) = \sum_{j=1}^{m} 4\pi \left[\kappa_j a_j (T_s) \frac{\partial I_b}{\partial T}\bigg|_{T_s} \phi(Z) + \frac{\partial \kappa_j a_j}{\partial T}\bigg|_{T_s} I_b(T_s)\phi(Z) \right] - \kappa_j G_j \tag{21}$$

and

$$G_j = \sum_{l=1}^{n} I_j' \phi(Z) \tag{22}$$

is the irradiation over 'n' number of discrete directions.

Critical parameters (critical Rayleigh number, Ra_c, and critical wave number, k_c) are obtained by quadratic search method for the marginally stable curve (for eigenvalue with zero real part), by solving the eigenvalue problem (Eq. 15), using the total radiative disturbance equation 21 and stability equations (Eqs. 12 and 13).

4. Results and discussion

4.1 *Verification of present numerical results*

Linear stability analysis of the Rayleigh–Benard problem for gray and non-gray participating media is studied numerically. The set of stability equations are also solved by the analytical Chebyshev spectral collocation method. For the case of non-radiating fluid (corresponding to the limit of $Pl \to \infty$), the marginally stable curve depicted in figure 2 is calculated using five Chebyshev polynomial expansion terms for the stability equations (Eqs. 12 and 13) and the corresponding critical Rayleigh number and wave number are 1707.96 and 3.10, respectively.

Stability curve for a gray participating medium is also shown in figure 2, at 800 K mean temperature and optical thickness of 0.09 with black boundaries. The

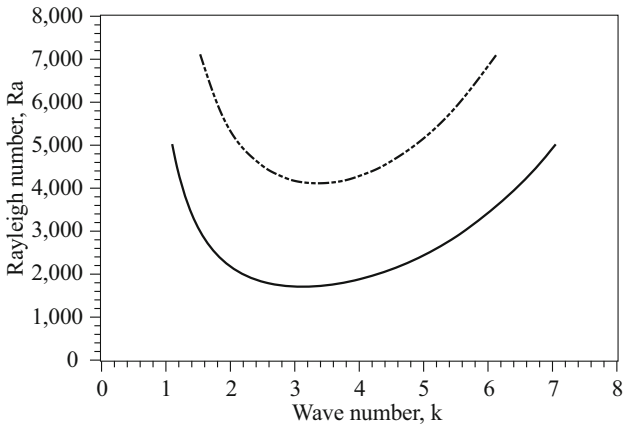

Figure 2. Marginal stability curve for radiating fluid (broken line) for optical thickness of 0.09 with black walls. The corresponding marginal stability curve for non-radiating fluid is shown as a continuous line.

figure illustrates that the critical Rayleigh number is 4012.4, and 3.39 is the corresponding wave number for the radiatively participating medium. Comparatively, the classical values for the non-radiating fluid are Ra_c = 1708 and K_c = 3.11. It is evident that in a radiatively participating medium convective instability is delayed to a larger Rayleigh number, because a significant fraction of heat transfer is carried out by radiation than by conduction. Thus, the fluid layer stability is enhanced in the presence of radiation as compared with the case of a non-participating medium.

The present numerical procedure including the spectral method for normal mode analysis and radiative flux evaluation by finite-volume-based discrete ordinates method has been validated with the semi-analytical results of Bdeoui and Soufiani [9] for a gray participating medium with varying parameter values of $3\tau^2\chi$. Here, the non-dimensional parameter χ is defined as $\chi = \dfrac{16\sigma T_0^3}{3\kappa k_T}$ and the results are summarized in table 1. It may be noted here that in the generalized numerical scheme for evaluating the radiation flux term, the number of gray gases 'm'is set as unity for the validation problem involving a gray gas. Good match is observed between the earlier analytical-method-based results and the present results, thereby validating the numerical solution methodology. Additionally, the results are compared with the results of Lan *et al* [12] for the experimental data independently reported by Gille and Goody [4] and Hutchison and Richards [10] in table 2. The participating medium consists of ammonia and carbon dioxide and the radiative properties are calculated from the Hottel's chart [24] at 580 and 800 K, respectively. For water vapor, at 500 K mean temperature, the critical Rayleigh number and wave number values reported by Bedeoui and Soufiani [9] using correlated-k (CK) model for absorption coefficient variation are also compared with the present critical parameter values obtained using SLW model, as shown in table 3. For all the cases considered, the present results are reasonably close to the published results. The minor variations, observed between the present numerical predictions and those of other research works listed in tables 1–3, can be attributed to the fact that actually reported radiative property data for gray/non-gray gases at different temperatures are deployed in the present study. In most of the other studies, radiative property values of comparative magnitudes have been clubbed in the form of specified non-dimensional numbers. It is important to incorporate actual property variations to obtain more realistic predictions.

Table 2. Comparison of present results with the results of Lan *et al* [12] for ammonia (NH_3) and carbon dioxide (CO_2) medium at 580 and 800 K, respectively, with black walls.

	Ref. [12]	Present results	
Medium	Ra_c	Ra_c	k_c
NH_3	2125	2088.43	3.22
CO_2	2050	2009.85	3.2

4.2 *Effect of mean temperature on the convective stability of the fluid layer*

Non-dimensionalizing the radiative heat flux q_r by σT_0^4 and length by κ^{-1} (where κ is the absorption coefficient), Eq. (5) can be written in non-dimensional form as

$$Pl\frac{d^2T^*}{dZ^{*2}} = \frac{dq_r^*}{dZ^*} \tag{23}$$

where the Planck number is defined as $Pl = \dfrac{\kappa k_T}{4\sigma T_0^3}$. It is evident that $Pl \gg 1$ denotes conduction-dominated regime and $Pl \ll 1$ represents radiation-dominated situation. The radiation-dominated regime is realized for large mean temperature (T_0) values and this leads to the radiative equilibrium condition that is a special case of Eq. (23), when the left hand side is completely neglected, i.e. conduction heat transfer is ignored. In this case, the equation leads to the expression

$$\frac{dq_r^*}{dZ^*} = 0. \tag{24}$$

The static solution for this equation is the self-adjusted temperature distribution depending on the optical thickness

Table 1. Comparison of present results with the results of Christophorides and Davis [6] and Bdeoui and Soufiani [9] for gray medium with black walls.

		Ref. [6] (semi-analytical)		Ref. [9] (semi-analytical)		Present results (numerical)	
$3\tau^2\chi$	Initial temp. profile	Ra_c	k_c	Ra_c	k_c	Ra_c	k_c
1	linear	1794.14	3.17	1792.66	3.17	1832.39	3.2
5	(with –0.5 gradient)	2127.42	3.33	2112.02	3.33	2182.93	3.36
1	exact solution	–	–	1838.88	3.17	1892.27	3.21
5	(from Eq. 5)	–	–	2358.03	3.33	2383.9	3.25

Table 3. Comparison of present results with the results of Bdeoui and Soufiani [9] for non-gray water vapor medium at 500 K with black walls.

Ref. [9]				Present results	
Linear stability theory		Numerical simulation		Numerical linear stability	
Ra_c	k_c	Ra_c	k_c	Ra_c	k_c
5232.24	3.57	5426	3.74	5589.58	3.74

of the medium and wall emissivity. For the radiative equilibrium case, the linear stability is applied and the perturbed radiative flux divergence (Eq. 21) is solved for the static self-adjusted temperature profile resulting from Eq. (24). The present case provides one of the two limiting cases, i.e. conduction limit (classical Rayleigh–Benard problem for $Pl \to \infty$) and the radiative equilibrium limit in the absence of conduction ($Pl = 0$). For the case with $k_T = 0$, the Rayleigh number is modified by replacing the medium thermal conductivity by $\sigma T_0^3/\kappa$. The modified Rayleigh number is expressed as

$$Ra_r = \frac{g\beta\Delta T L^3}{\left(4\sigma T_0^3 \nu/\kappa\rho c_p\right)}. \tag{25}$$

Since radiation heat transfer is a strong function of temperature, the stability of radiative equilibrium can vary strongly with the mean temperature T_0. Simulations have been performed for this limiting case with varying mean temperature values for black as well as gray bounding walls. The corresponding critical Rayleigh numbers ($Ra_{r,c}$) and wave numbers ($k_{r,c}$) are summarized in table 4.

It is evident from table 4 that the fluid layer stability decreases at higher medium temperature, as radiative heat flux increases. However, if the net radiation flux decreases due to reflection at the wall boundary, the critical values $Ra_{r,c}$ and $k_{r,c}$ increase for the case of wall emissivity ϵ_w = 0.5, as compared with the case of black walls ($\epsilon_w = 1$). The radiation-property-based critical Rayleigh number and wave number ($Ra_{r,c}$ and $k_{r,c}$) decrease with T_0, implying greater propensity for the onset convection. Earlier studies (Ref. [9]) have predicted results only where the layer stability increases with mean fluid temperature, in the presence of volumetric radiation, for cases that are conduction dominated. For the first time the present results (both exact solutions and numerical predictions) show that the stability of the layer against the onset of convection decreases at higher mean temperature, in the radiation-dominated regime.

Further, for conduction–radiation heat transfer in a gray participating medium with an optical thickness of 0.1 and 0.4, the critical Rayleigh number and wave number variations with mean temperature values are shown in figure 3. The Ra_c and k_c values decrease with increase in mean

Table 4. Effect of mean temperature on critical values for the case of radiative equilibrium for wall emissivity (ϵ_w) of 1 and 0.5 and optical thickness of 1.74.

	$\epsilon_w = 1$		$\epsilon_w = 0.5$	
Temperature (K)	$Ra_{r,c}$	$k_{r,c}$	$Ra_{r,c}$	$k_{r,c}$
500	9061.17	3.97	13150.3	3.83
600	6585.17	3.8	9910.29	3.66
700	5253.07	3.65	8282.13	3.52
800	4531.1	3.52	7813.83	3.4

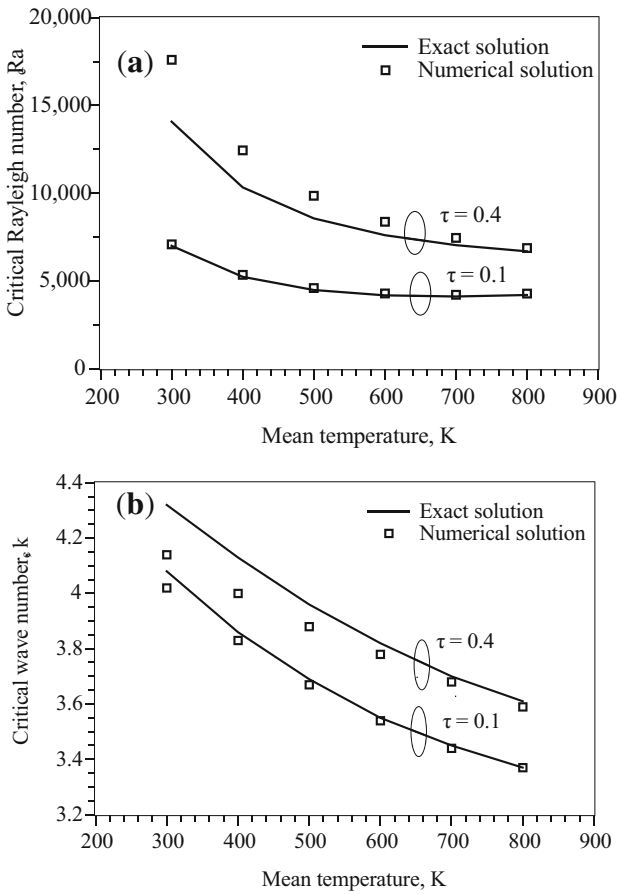

Figure 3. Variation of critical (a) Rayleigh number and (b) wave number with mean temperature values for optical thickness of 0.1 and 0.4; comparison of exact and numerical results with $\epsilon_w = 1$ is also shown.

temperature values as a result of the increase in radiation heat transfer (discussed earlier) and figure 3 also shows the comparison of exact and numerical results for both optical thickness cases. Here, the exact results are obtained by optical thin approximation for which the perturbed radiative flux divergence is given as

$$Q(Z) = 16\sigma\kappa T_s^3(Z)\phi(Z). \tag{26}$$

Here, the amplitude function $\phi(Z)$ is expanded as a Chebyshev polynomial series. A 10-term expansion provides results that converge within an error tolerance of 10^{-5}, for the exact solution. In figure 3, the exact solution underpredicts critical Rayleigh number and wave number at higher optical thickness value (0.4); however, at lower optical thickness value (0.1), the exact and numerical solutions are in excellent match. This can be attributed to the optical thin approximation used for calculating perturbed divergence of radiative flux (Eq. 26, for $\tau \ll 1$) as compared with Eq. (21). Figure 4 shows the corresponding temperature distribution for a typical mean temperature of 300 and 600 K for both optical thickness values (0.1 and 0.4). Firstly, for a given optical thickness, increase in mean temperature increases the radiation heat transfer in the cavity that results in a steep temperature gradient near the walls and thus advances the onset of natural convective flow, i.e. decrease in critical parameter values with increase in mean temperatures. On the other hand, for fixed mean temperature, increase in optical thickness results in a nonlinear temperature profile due to increase in emission and absorption through the medium; thus the stability of the fluid layer increases with increase in the critical parameter values (figures 3a and 3b). Both exact and numerical temperature distributions shown in figures 4a and 4b, respectively, follow similar behaviors, as discussed earlier. After this validation exercise the numerical methodology has been followed for further studies.

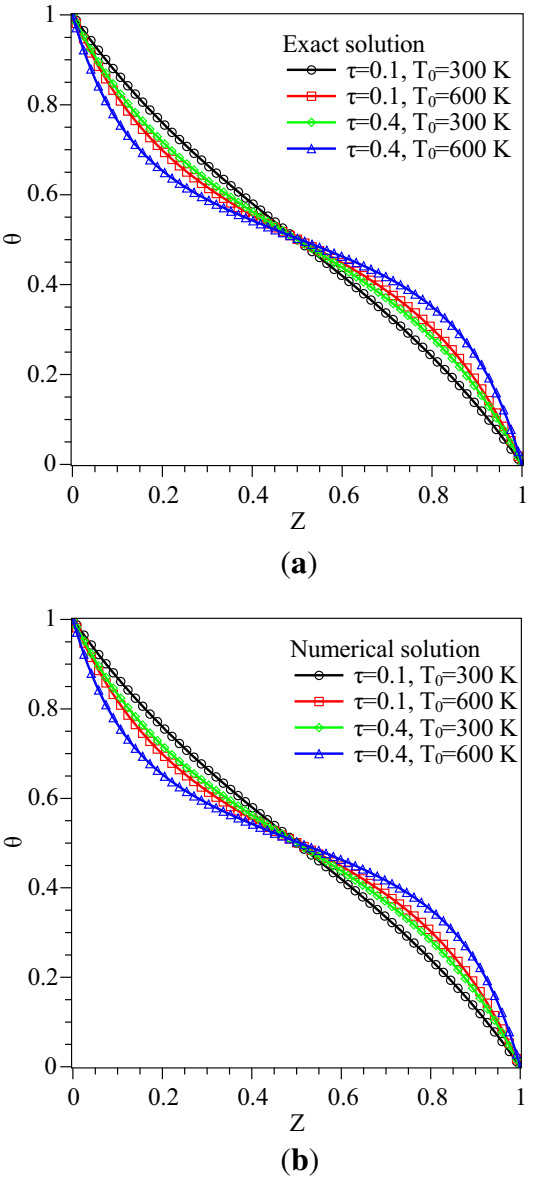

Figure 4. Temperature distribution in a 5 cm gray fluid layer: (a) exact and (b) numerical, for two optical thicknesses and mean temperature values ($\tau = 0.1, 0.4$ and $T_0 =$ 300, 600 K) with $\epsilon_w = 1$.

4.3 *Effect of Planck number on the stability of a gray radiating fluid*

The mean operating temperature (T_0) strongly affects the volumetric radiation process, which, in turn, changes the temperature distribution in the medium. The temperature distributions for various mean temperature values are shown in figure 5. The basic steady state solution (Eq. 5), is determined by the combined conduction–radiation heat transfer governed by the Planck number. It is defined as the ratio of conduction to radiation heat transfer and expressed as $Pl = \dfrac{\kappa k_T}{4\sigma T_0^3}$. For typical mean temperature values of 500, 600, 700 and 800 K, the corresponding Planck number values are found to be 0.0203, 0.0145, 0.0108 and 0.0008, respectively. As seen from the definition of *Pl*, radiation dominates in the combined conduction and radiation heat transfer for decreasing values of Planck number.

In a non-radiating fluid, heat transfer changes from pure conduction regime to conduction–convection regime after the onset of convection. In a radiating fluid the system changes from conduction–radiation regime to conduction–radiation–convection regime, by the onset and evolution of a convective flow. The critical Rayleigh number and wave number variations with Planck number are shown in figure 6 for an optical thickness value of 0.87 with black bounding surfaces. Figure 6 shows that for a high value of Planck number, where conduction heat transfer dominates

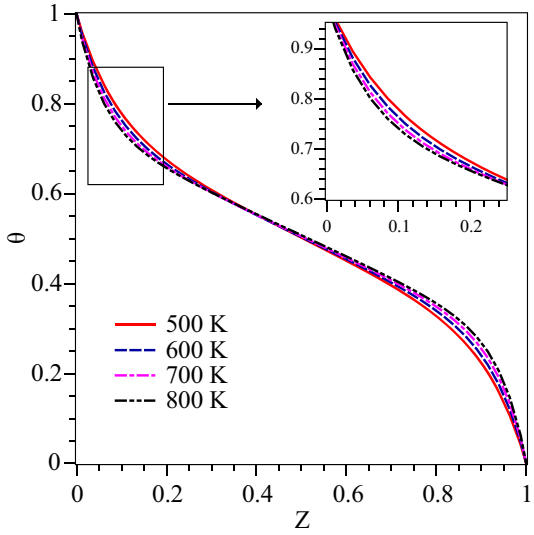

Figure 5. Temperature distribution in a gray participating medium for various mean temperatures.

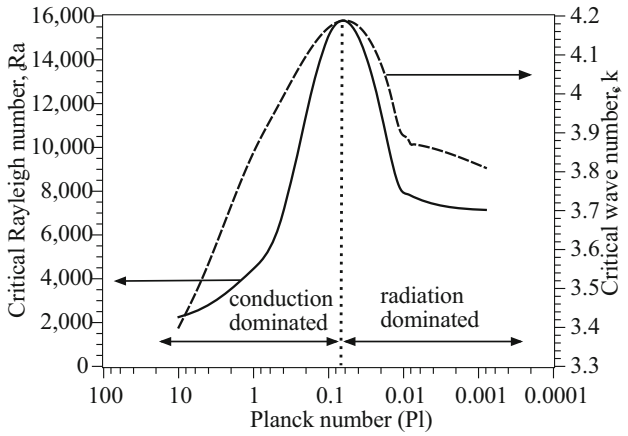

Figure 6. Critical Rayleigh number and wave number variations with Planck number for optical thickness of 0.87 for a gray medium bounded by black walls.

over radiation, the flow critical values asymptotically approach the conduction limits as $Pl \to \infty$, i.e., $Ra_c = 1708$ and $k_c = 3.11$. However, these values increase with decrease in Planck number as radiation heat transfer also makes a significant contribution and increases the fluid layer stability against the onset of convection. Below a certain value of Planck number, the critical $Ra_c (= g\beta\Delta TL^3/\nu\alpha)$ and k_c decrease with decrease in Planck number. For a given set of data, maximum stability is attained around $Pl \approx 0.1$. Finally, when $Pl \to 0$, the situation tends towards the radiative equilibrium case, with conduction heat transfer becoming negligible. Similar cases of low Planck number values (radiation dominated) are encountered in the present study for gray and non-gray participating media.

For the temperature distribution shown in figure 5, both the critical Rayleigh number and wave number decrease with decrease in Planck number due to the significant changes occurring in the temperature distribution because of the radiation source term. Also, the associated temperature gradient increases adjacent to the walls and the system becomes sensitive to small temperature disturbances (propensity for the onset of convective instability increases) at higher mean temperature values. Figures 5 and 6 illustrate that even for a gray medium the critical parameters change drastically with mean temperature T_0, due to shift in heat transfer from conduction-dominated to radiation-dominated regimes and the associated changes in the temperature profiles.

In the radiative equilibrium limit (in the absence of conduction heat transfer) a temperature slip occurs close to the boundaries. In this limit, the initial self-adjusted temperature distribution is used and the system response is analyzed for small perturbations added to this self-adjusted temperature distribution. The results shown in table 4 are obtained for the radiative equilibrium case by considering the temperature slip close to the boundaries. For the case of combined conduction–radiation heat transfer, the initial temperature distribution is of continuous nature that satisfies Eq. (23). Table 5 illustrates the effect of temperature slip close to the boundaries for radiative equilibrium case and combined conduction–radiation case. It is seen from the table that the presence of conduction heat transfer increases the stability of the layer to higher Rayleigh number as compared with radiation alone, thus highlighting the influence of temperature slip close to the boundaries.

Table 6 shows the effect of wall emissivity on the onset of natural convection. At high Planck number ($Pl \gg 1$) values the radiative heat flux between the walls decreases for the case of $\epsilon_w = 0.1$ as compared with that of black walls, at fixed wall temperatures. Reduction in radiation heat transfer relatively increases the conduction heat transfer contribution and thereby reduces the stability of the fluid layer. It is seen that Ra_c decreases slightly when wall emissivity ϵ_w is reduced, for the conduction-dominated

Table 5. Effect of temperature slip for the case of radiative equilibrium and combined conduction–radiation case for optical thickness 1.74 with black bounding surfaces ($\epsilon_w = 1$).

	Equilibrium case (slip)		Combined conduction–radiation case (no-slip)	
T_0	Ra_c	k_c	Ra_c	k_c
500	9061.17	3.97	11708.5	4.08
600	6585.17	3.8	9440.3	3.99
700	5253.07	3.65	8052.4	3.9
800	4531.1	3.52	7144.3	3.81

Table 6. Critical parameters for the onset of convection at different wall emissivities (optical thickness = 1.74).

	$\epsilon_w = 1$		$\epsilon_w = 0.1$	
Pl	Ra_c	k_c	Ra_c	k_c
10	2251.56	3.4	2217.29	3.4
5	2627.43	3.52	2575.38	3.52
1	4461.36	3.85	4431.6	3.8
0.5	6047.53	3.96	6268.3	3.87
0.1	15092.8	4.17	23466.8	4.45
0.0203	11708.5	4.08	24620.3	4.05
0.0145	9440.3	3.99	18567.4	4.03
0.0108	8052.4	3.9	15673.3	3.92
0.0008	7144.3	3.81	14538.8	3.78

cases ($Pl \gg 1$). On the other hand, in the radiation-dominated cases, higher contribution of radiation (with increase in *Pl*) renders the fluid layer more unstable with reference to the onset of convection, Hence, for $Pl \ll 1$, the case of $\epsilon_w = 0.1$, which leads to lower radiation heat flux as compared with the case of black walls (due to wall reflections), increases the stability of the layer. Hence, Ra_c for $\epsilon_w = 0.1$ is higher than that for $\epsilon_w = 1$ when other parameters are maintained the same.

4.4 *Stability analysis of a non-gray medium*

For a gray medium, the absorption coefficient is constant and only the black body emissive power induces disturbance due to perturbation in temperature. However, for a non-gray medium, disturbance growth is more complex, since the absorption coefficient itself becomes a strong function of temperature, mole fraction of gas species and operating pressure. SLW is a suitable model that takes into account such dependence. The detailed methodology and application of SLW model to radiation problems can be found in earlier studies [22, 23]. For a homogeneous medium at atmospheric pressure, the absorption coefficient and corresponding black body weights become functions of temperature only. The corresponding volumetric radiative power disturbance term is evaluated from Eq. (21) due to temperature perturbations. For non-gray carbon dioxide and water vapor media, temperature distribution for steady state is shown in figure 7. The corresponding critical Ra_c values are shown in figures 8a–d. The medium consists of pure carbon dioxide (figure 7a) and pure water vapor (figure 7b) with black boundaries, at various mean temperatures. It is seen that the mean temperature substantially affects the temperature distribution for water vapor medium due to its stronger emission and absorption characteristics for thermal radiation. However, the mean temperature has only a relatively weaker effect for carbon dioxide. It is evident that at higher mean temperatures of the layer the gradient of temperature becomes steeper near the walls, with the mid-portion of the layer being stratified.

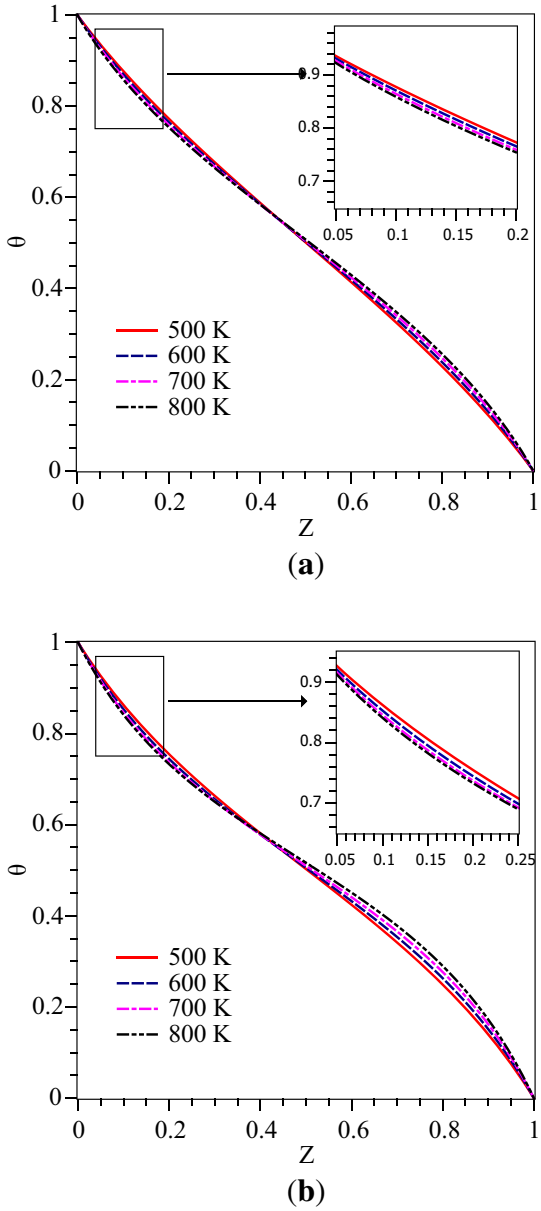

Figure 7. Non-dimensional temperature distribution for non-gray media bounded by black walls: (a) pure carbon dioxide and (b) pure water vapor.

Figure 8 shows the variations of critical Rayleigh number and wave number with mean temperature for SLW and Planck model (κ_P). Planck mean absorption coefficient evaluated at mean temperature is represented as [25]

$$\kappa_P = \sum_{j=1}^{m} a_j \kappa_j. \tag{27}$$

The medium consists of either water vapor or carbon dioxide with wall emissivity of 1 and the top and bottom

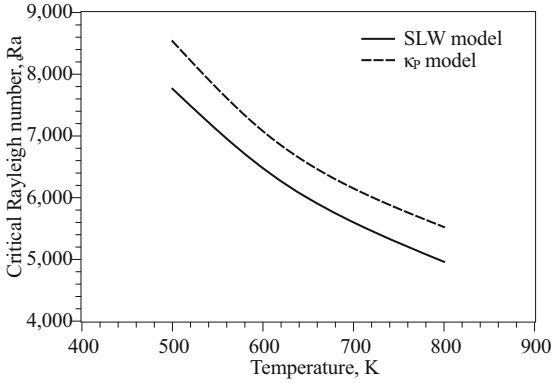

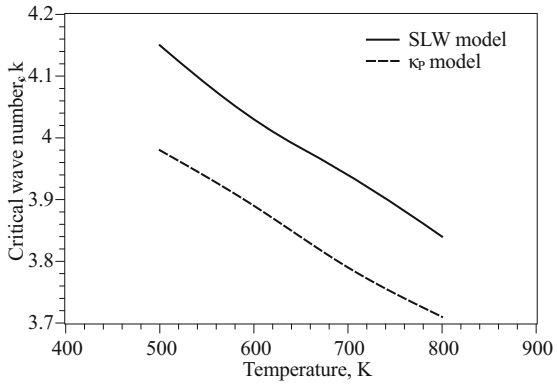

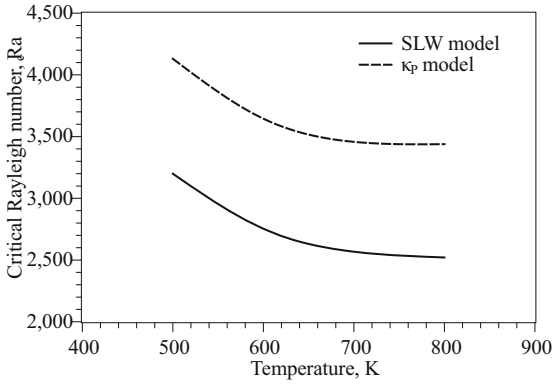

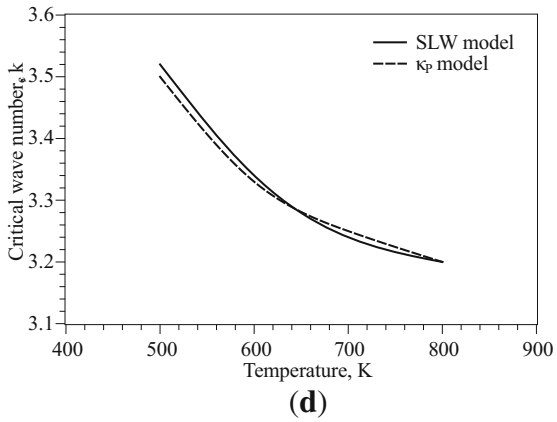

◀**Figure 8.** Critical Rayleigh number and wave number comparison between SLW model and Planck model (κ_P) in a 4 cm layer of CO_2 ((a) and (b)) and H_2O ((c) and (d)).

walls are separated by a distance of 4 cm. The critical Rayleigh number and wave number decrease with temperature for both H_2O and CO_2 and the values predicted by the SLW model fall below those of the Planck model due to the temperature-dependent absorption coefficient and weight factors. Also, water vapor shows greater sensitivity to the model employed than carbon dioxide for the onset of convective motion. The Planck model with a constant mean absorption coefficient evaluation at mean temperature also follows similar trends as the more elaborate SLW model, which considers more realistic estimation of radiative properties. However, noticeable differences exist between these two models.

For a non-gray medium the Static Heat Flux Ratio (*SHFR*), which is the ratio of conduction to radiation heat transfer, is defined as

$$SHFR = \frac{q_c}{q_r}. \tag{28}$$

The *SHFR* values for H_2O medium are 0.081, 0.064, 0.052, 0.042 and the corresponding values for CO_2 are 0.043, 0.034, 0.028, 0.023 at the mean temperature values of 500, 600, 700 and 800 K, respectively. *SHFR* is similar to Planck number for a gray medium and it decreases with increase in mean temperature as radiation heat transfer becomes dominant over heat conduction. Since water vapor exhibits wider absorption bands, the critical *Ra* values for water vapor are lower in comparison with those of carbon dioxide. In other words the temperature profile is more non-linear in the case of water vapor, which advances the onset of convection to a lower Ra_c value.

Figure 9 shows the non-dimensional static temperature distribution for pure H_2O (figure 9a) and pure CO_2 (figure 9b) for black and gray ($\epsilon_w = 0.1$) bounding surfaces. At the boundaries the radiation flux changes substantially due to change in wall emissivity, which, in turn, alters the temperature distribution significantly. In addition to this, for the boundary conditions of black walls, the mole fraction of the radiatively active species is varied from 1 to 0.1 (with other species being nitrogen), and the corresponding temperature profiles are shown in figure 10. With decrease in mole fraction of the radiatively active gas species, the medium becomes transparent to radiation and the temperature distribution changes from non-linear to a nearly linear form when the mole fraction approaches zero. The corresponding temperature profiles for varying mole fraction of H_2O and CO_2 are shown in figures 10a and 10b, respectively.

Table 7 shows the effects of wall emissivity and mole fraction variations on critical Rayleigh number and wave

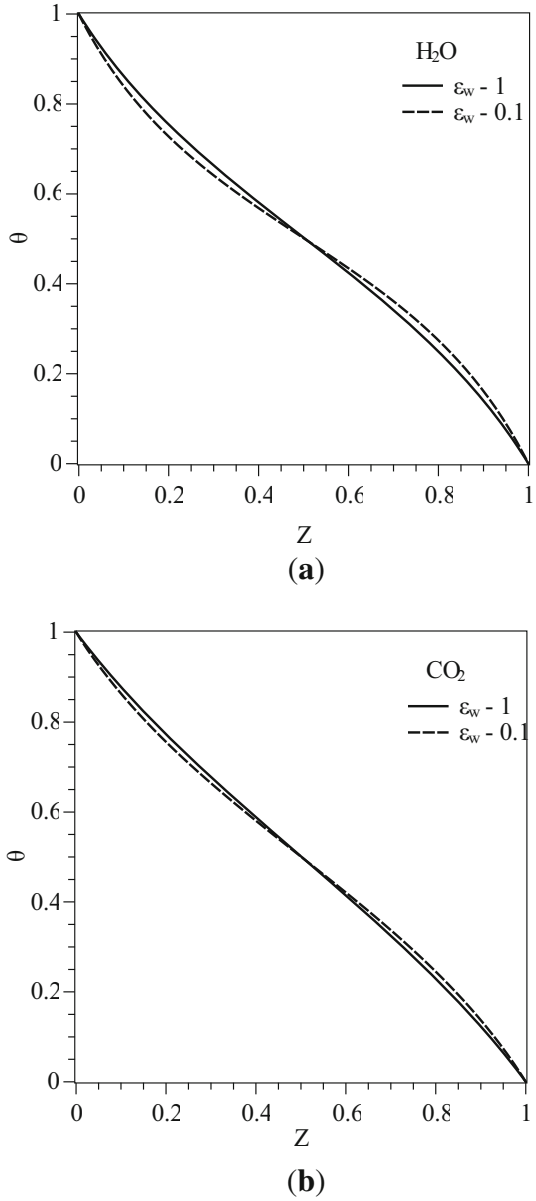

Figure 9. Effect of wall emissivity on static non-dimensional temperature distribution at 500 K in a 4 cm layer of (a) H_2O and (b) CO_2.

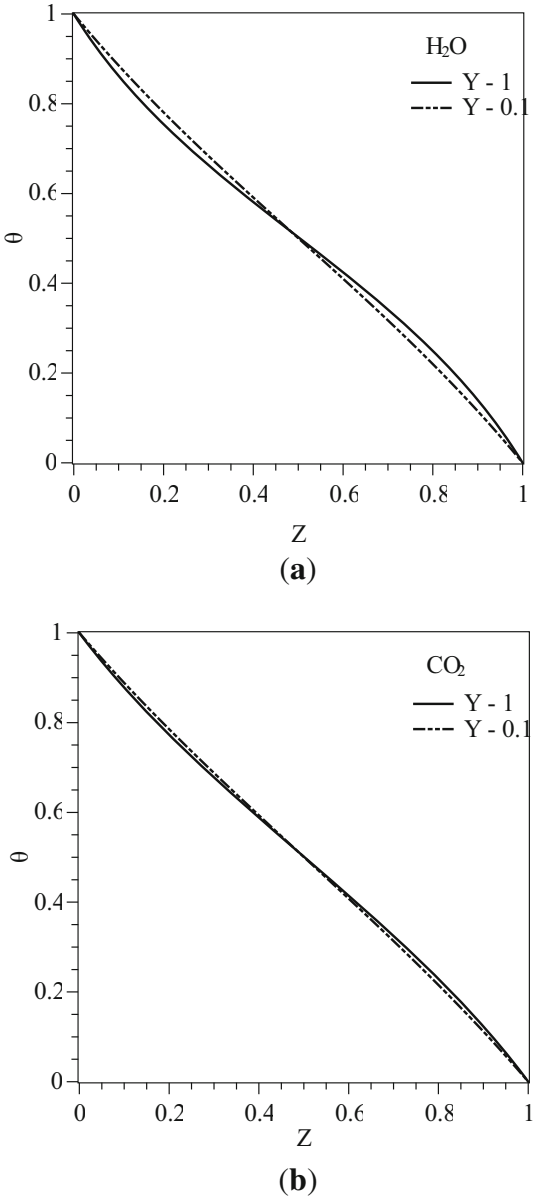

Figure 10. Effect of species mole fraction variation on static non-dimensional temperature distribution at 500 K in a 4 cm layer of (a) H_2O and (b) CO_2.

number at 500 K mean temperature in a 4 cm fluid layer. The wall emissivity values influence the temperature distribution through boundary intensity variation and divergence of radiative heat flux. The change in wall emissivity from 1 (completely absorbing) to 0.1 (partially absorbing and reflecting) increases the critical Rayleigh number due to the reflection of radiation flux at the boundaries. Further, the mole fraction of the radiatively active gas species (H_2O or CO_2) is varied from 1 to 0.1 for black walls. Decreasing the mole fraction of H_2O or CO_2 reduces the critical Rayleigh number substantially and it asymptotically approaches the conduction limit, i.e. 1708 (with a wave number value of 3.11), as a result of reduction in the volumetric radiation flux in the gas medium. Increase in the critical Rayleigh number value implies greater stability of the conduction–radiation heat transfer situation, against the onset of convection.

4.5 *Stability analysis of non-gray medium: mixture of gases*

For results presented in the preceding section, the medium was considered to consist of either carbon dioxide or water vapor along with nitrogen. In the mixture, nitrogen is essentially neutral to the volumetric radiation process. If all

Table 7. Critical Rayleigh number and wave number values for varying wall emissivity and mole fraction of CO_2 and H_2O at 500 K mean temperature.

	Mole fraction (Y_i)			Critical values	
ϵ_w	H_2O	CO_2	N_2	Ra_c	k_c
1	1	–	–	3199.28	3.52
1	–	1	–	7764.5	4.15
0.1	1	–	–	3560.55	3.5
0.1	–	1	–	8094.13	4.16
1	0.1	–	0.9	2041.47	3.24
1	–	0.1	0.9	2420.29	3.43
1	0.5	–	0.5	2723.55	3.42
1	–	0.5	0.5	4651.02	3.82

the three gases, i.e. carbon dioxide, water vapor and nitrogen, coexist, the stability analysis of such a system can become complex.

SLW approach for a multi-component gas mixture is modeled by following Solovjov and Webb [26]. They have proposed various solution techniques for multi-component gas mixtures such as convolution method, superposition method and multiplication method, and compared the results to the line-by-line benchmark solution. In the present work, multiplication approach has been used because of its simplicity and application to a wide range of radiation problems. In this method, the multi-component gas mixture is assumed to be homogeneous and behaves as a single gas species. The absorption line black body distribution function is generated for the gas mixture by taking into account fine spectral variation of absorption coefficient of individual gas component and correspondingly evaluating the absorption coefficient and weight factors. Here, the mole fractions of individual gas species play an important role with respect to the radiation calculations. Typical variation of absorption cross-section with wave number is shown in figure 11 for H_2O and figure 12 for CO_2 and the effect of temperature on absorption cross-section is also seen, which is quite significant. A comparison of the absorption cross-sections for the two gases at 500 K temperature is depicted in figure 13, which shows wide differences in absorption behavior of H_2O and CO_2. Due to these differences, the divergences of radiative flux, temperature distribution and overall stability of the system are modified significantly.

For a mixture of gases (H_2O, CO_2 and N_2), the static temperature distribution is shown in figure 14 for black walls and for varying mole fraction of gas species. A comparison of the temperature profiles for a mixture with 0.1, 0.1 and 0.8 mole fractions of H_2O, CO_2 and N_2 with another mixture of 0.5, 0.5 and 0.0 mole fractions for the respective species is presented. The temperature profile for the mixture with high nitrogen fraction (0.8) is nearly linear

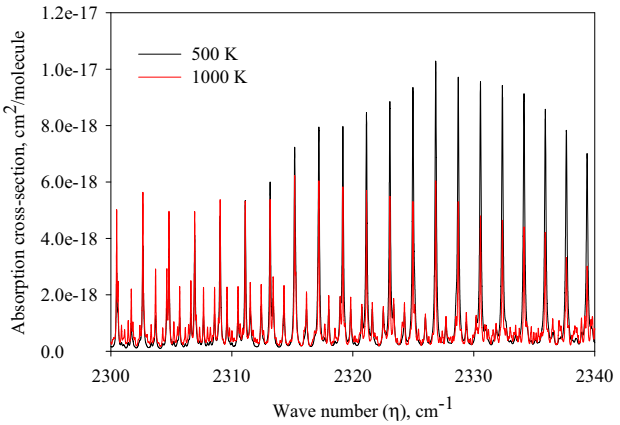

Figure 12. Absorption cross-section variation with wave number for CO_2 at 500 K (black) and 1000 K (red) temperatures (η range of 2300–2340 cm^{-1}).

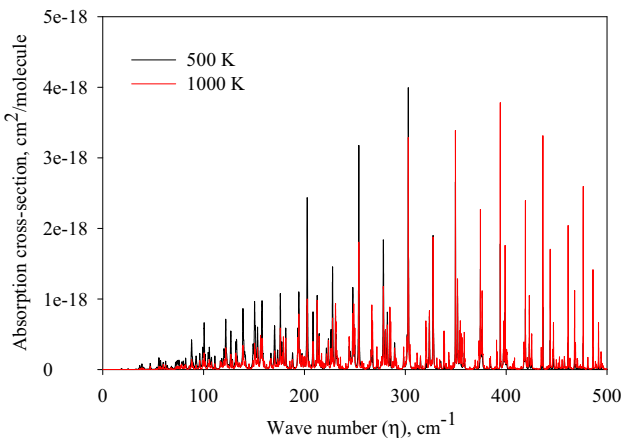

Figure 11. Absorption cross-section variation with wave number for H_2O at 500 K (black) and 1000 K (red) temperatures (η range of 0–500 cm^{-1}).

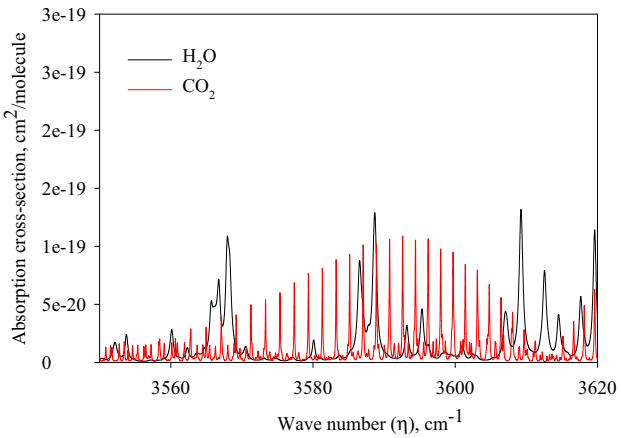

Figure 13. Comparison of absorption cross-section variation with wave number for H_2O (black) and CO_2 (red) at 500 K temperature (η range of 3500–3620 cm^{-1}).

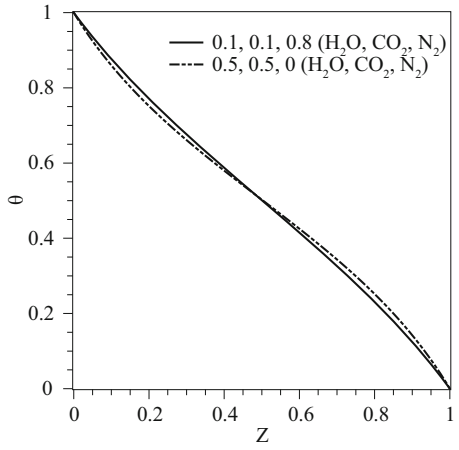

Figure 14. Static non-dimensional temperature distribution in a mixture of gases for (a) 0.1, 0.1, 0.8 mole fraction of H_2O, CO_2, N_2, respectively, and (b) 0.5, 0.5, 0 mole fraction of H_2O, CO_2, N_2, respectively, at 500 K and $\epsilon_w = 1$.

Table 8. Critical Rayleigh number and wave number values for gas mixtures with varying wall emissivity and mole fraction values of CO_2 and H_2O at 500 K mean temperature.

	Mole fraction (Y_i)			Critical values	
ϵ_w	H_2O	CO_2	N_2	Ra_c	k_c
1	0.1	0.1	0.8	2722.4	3.47
1	0.5	0.5	0	5322.3	3.94
0.5	0.1	0.1	0.8	2797.33	3.45
0.5	0.5	0.5	0	5590.86	3.87
1	0.9	0.1	0	3634.18	3.61
1	0.1	0.9	0	7340.67	4.1

and the profile for the mixture of 0.5 H_2O, 0.5 CO_2 is non-linear.

Effect of species mole fractions on the critical Rayleigh number is summarized in table 8 for a 4 cm thick medium at 500 K mean temperature. For a mixture of gases (CO_2, H_2O and N_2) the spectral absorption coefficient of each gas influences the absorption behavior of the mixture, because of the overlap of absorption lines in the radiation spectrum. The critical Rayleigh number predicted for a mixture of 0.1 mole fraction of CO_2 and H_2O each with 0.8 mole fraction of N_2, enclosed by black bounding surfaces, is found to be 2722.4. The critical Rayleigh number for 0.1 mole fraction of H_2O and 0.9 mole fraction of N_2 is 2041.47 and the corresponding value for 0.1 mole fraction of carbon dioxide and 0.9 mole fraction of N_2 is 2420.29. Thus, the mixture behavior is very different with respect to the convective instability as compared with the individual behavior of the corresponding gases. The emission and absorption characteristics of gas mixture change due to the overlap of absorption lines in the spectrum and the effect of such overlap on the critical Rayleigh number value is evident. The critical Rayleigh number increases with increase in the mole fraction of CO_2 and H_2O to 0.5 each, as compared with the case with lower mole fraction of these species. If the wall emissivity for the gas mixture is changed from 1 to 0.5, the corresponding critical Rayleigh number is increased due to partial absorption and reflection of radiation flux at the boundaries.

Observing the values of the critical parameters carefully for a mixture of gases, it is found that the mixture behavior varies linearly with the composition of individual gases where only radiatively participating gases are present. Such a behavior can be expressed as a linear interpolation of the form

Table 9. Comparison of critical parameters from linear stability theory and linear interpolation model for varying mole fraction of gases at 500 K and $\epsilon_w = 1$.

Mole fraction			Linear stability theory		Linear interpolation model		Change (%)	
Y_{H_2O}	Y_{CO_2}	Y_{N_2}	Ra_c	k_c	Ra_c	k_c	Ra_c	k_c
1	0	0	3199.28	3.52	3199.28	3.52	0	0
0.9	0.1	0	3634.18	3.61	3655.8	3.58	0.59	0.75
0.75	0.25	0	4213.34	3.72	4340.58	3.67	3.02	1.26
0.6	0.4	0	4842.09	3.83	5025.36	3.77	3.79	1.39
0.5	0.5	0	5322.3	3.94	5481.89	3.83	3	2.66
0	1	0	7764.5	4.15	7764.5	4.15	0	0
0.1	0.9	0	7340.67	4.1	7307.97	4.08	0.45	0.32
0.25	0.75	0	6550.31	4.02	6623.19	3.99	1.11	0.68
0.4	0.6	0	5794.08	3.94	5938.41	3.89	2.49	1.07
0.1	0.1	0.8	2722.4	3.47	2462.77	3.25	9.54	6.20
0.1	0	0.9	2041.47	3.24	1857.12	3.15	9.03	2.75
0	0.1	0.9	2420.29	3.43	2313.65	3.21	4.41	6.3
0.5	0	0.5	2723.55	3.42	2453.64	3.31	9.91	3.07
0	0.5	0.5	4651.02	3.82	4736.25	3.63	1.83	4.97

$$Ra_c = Ra_{c,0} + Y_{H_2O}\Delta Ra_{c,H_2O} + Y_{CO_2}\Delta Ra_{c,CO_2} \quad (29)$$

$$k_c = k_{c,0} + Y_{H_2O}\Delta k_{c,H_2O} + Y_{CO_2}\Delta k_{c,CO_2} \quad (30)$$

where $Ra_{c,0}$ and $K_{c,0}$ are the critical Rayleigh number and wave number for non-radiating fluid (i.e. 1708 and 3.11, respectively). The expression $\Delta Ra_{c,H_2O}$ is the difference between critical Rayleigh number for pure H_2O and for non-radiating fluid calculated as $\Delta Ra_{c,H_2O} = Ra_{c,H_2O} - Ra_{c,0}$, and for CO_2 as $\Delta Ra_{c,CO_2} = Ra_{c,CO_2} - Ra_{c,0}$. Similarly, the wave number differences are calculated as $\Delta k_{c,H_2O} = k_{c,H_2O} - k_{c,0}$, $\Delta k_{c,CO_2} = k_{c,CO_2} - k_{c,0}$ for H_2O and CO_2, respectively. Comparison of critical parameters obtained from the linear interpolation model and linear stability theory is summarized in table 9. For a medium consisting of only radiatively active gases, the proposed linear interpolation model predicts the critical Rayleigh number and wave number with maximum error of 3.8% in comparison with the linear stability theory. On the other hand, the error increases up to 10% when a non-participating gas like nitrogen is included.

5. Conclusion

Rayleigh–Benard type convection instability in the presence of gray and non-gray participating media is studied numerically. The spectral Chebyshev collocation method is used to solve the linear stability equations and the SLW model is utilized to evaluate the absorption coefficient of individual and mixture of non-gray gases numerically. The numerical methodology has high potential for studying convective instability over a wide range of boundary conditions, and for various radiative gas properties.

The results show that volumetric radiation in an absorbing-emitting medium stabilizes the layer against the onset of convection, thus leading to higher critical Rayleigh number, Ra_c, as compared with the situation of a radiatively non-participating medium. The radiatively participating medium offers an additional path for heat transfer between the walls, and the presence of radiative source term arising from the presence of absorbing and emitting medium increases the critical Rayleigh number limit. A radiatively participating medium also modifies the temperature distribution with steeper gradients near the walls and stratified fluid with weak gradients in the core region of the layer.

The mean temperature (T_0) of the medium strongly influences the stability of the system, resulting in higher Ra_c with an increase in the mean temperature at lower T_0 values (corresponds to high value of Planck number) and decrease in Ra_c at higher T_0 (corresponds to low value of Planck number). This can be attributed to the increase in the relative importance of radiation heat transfer as compared with conduction heat transfer at higher mean temperature values. Also, the magnitudes of temperature gradients near the hot and cold walls increase with T_0. At higher T_0 values, conduction heat transfer becomes insignificant and a regime of radiative equilibrium is approached. In this regime of $Pl \to 0$, instability of the layer for transition towards the onset of convection increases with mean temperature (i.e., Ra_c reduces with T_0). The wall emissivity significantly affects the stability of the medium by increasing the critical Rayleigh number with decrease in wall emissivity, as a result of reflected radiation in the radiation-dominated regime ($Pl \to 0$). However, in the conduction-dominated regime of $Pl \gg 1$, reduction in wall emissivity decreases Ra_c, as a result of reduction in the radiation contribution. With decrease in the mole fraction of radiatively participating gas species (CO_2 or H_2O), the volumetric radiation becomes insignificant and the value of Ra_c asymptotically approaches the classical value for a non-radiating fluid.

Nomenclature

C_p	specific heat at constant pressure, J/kg K
d	separation distance, m
G	total irradiation, W/m^2
g	acceleration due to gravity, m/s^2
I	total intensity of radiation, W/m^2 sr
k_T	thermal conductivity, W/m K
Pl	Planck number, $\frac{\kappa k_T}{4\sigma T_0^3}$
Pr	Prandtl number, $\frac{\nu}{\alpha}$
q	heat flux, W/m^2
Ra	Rayleigh number, $\frac{g\beta\Delta T d^3}{\nu\alpha}$
T	temperature, K
t	time, s
T_1, T_2	bottom and top wall temperature respectively, K
T_0	mean temperature, K
$\vec{V}$	velocity vector, $\vec{V} = u\vec{i} + v\vec{j} + w\vec{k}$
W	amplitude of velocity perturbation
Y	species mole fraction
Z	vertical distance, m

Greek letters

α	thermal diffusivity, m^2/s
α_s	non-dimensional static temperature gradient
ν	kinematic viscosity, kg/m-s
ρ	density, kg/m^3
κ	absorption coefficient, 1/m
Ω	solid angle, sr
ϵ	emissivity
θ	non-dimensional temperature field, $\theta = \frac{(T - T_c)}{(T_h - T_c)}$
ϕ	amplitude of temperature perturbation
σ	Stefan–Boltzmann constant, 5.67×10^{-8} W/m^2 K^4
τ	optical thickness, $\tau = \kappa L$

Subscripts

b black body
j non-gray gas index
c conduction mode
r radiation mode
s static condition
w wall

References

[1] Lord Rayleigh 1916 LIX. On convection currents in a horizontal layer of fluid, when the higher temperature is on the under side. *The London, Edinburgh, and Dublin Philosophical Magazine and Journal of Science* 32(192): 529–546

[2] Anne Pellew and Richard Vynne Southwell 1940 On maintained convective motion in a fluid heated from below. *Proceedings of the Royal Society of London A* 176(966): 312–343

[3] Sparrow E M, Goldstein R J and Jonsson V K 1964 Thermal instability in a horizontal fluid layer: effect of boundary conditions and non-linear temperature profile. *Journal of Fluid Mechanics* 18(4): 513–528

[4] John Gille and Richard Goody 1964 Convection in a radiating gas. *Journal of Fluid Mechanics* 20(1): 47–79

[5] Spiegel E A 1960 The convective instability of a radiating fluid layer. *The Astrophysical Journal* 132: 716

[6] Christophorides C and Davis S H 1970 Thermal instability with radiative transfer. *Physics of Fluids* 13(2): 222–226

[7] Arpaci V S and Doğan Gózúm 1973 Thermal stability of radiating fluids: the Bénard problem. *Physics of Fluids* 16(5): 581–588

[8] Lienhard J H 1990 Thermal radiation in Rayleigh–Bénard instability. *Journal of Heat Transfer* 112(1): 100–109

[9] Bdéoui F and Soufiani A 1997 The onset of Rayleigh–Bénard instability in molecular radiating gases. *Physics of Fluids* 9(12): 3858–3872

[10] Hutchison J E and Richards R F 1999 Effect of nongray gas radiation on thermal stability in carbon dioxide. *Journal of Thermophysics and Heat Transfer* 13(1): 25–32

[11] Mukutmoni D and Yang K T 1995 Thermal convection in small enclosures: an atypical bifurcation sequence. *International Journal of Heat and Mass Transfer* 38(1): 113–126

[12] Lan C H, Ezekoye O A, Howell J R and Ball K S 2003 Stability analysis for three-dimensional Rayleigh–Bénard convection with radiatively participating medium using spectral methods. *International Journal of Heat and Mass Transfer* 46(8): 1371–1383

[13] Wen Mei Yang 1990 Thermal instability of a fluid layer induced by radiation. *Numerical Heat Transfer* 17(3): 365–376

[14] Swaminathan Prasanna and Venkateshan S P 2014 Convection induced by radiative cooling of a layer of participating medium. *Physics of Fluids*, 26(5): 056603

[15] Larson V E 2001 The effects of thermal radiation on dry convective instability. *Dynamics of Atmospheres and Oceans* 34(1): 45–71

[16] Moufekkir F, Moussaoui M A, Mezrhab A, Naji H and Lemonnier D 2012 Numerical prediction of heat transfer by natural convection and radiation in an enclosure filled with an isotropic scattering medium. *Journal of Quantitative Spectroscopy and Radiative Transfer*, 113(13):1689–1704

[17] Dandy D S 2017 Chemical and Biological Engineering, Colorado State University, Colorado http://navier.engr.colostate.edu/∼dandy/code/code-2/index.html

[18] Subrahmanyan Chandrasekhar 2013 *Hydrodynamic and hydromagnetic stability*. Courier Corporation

[19] Claudio Canuto, Hussaini M Y, Alfio Quarteroni, Thomas Jr A *et al* 2012 *Spectral methods in fluid dynamics*. Springer Science & Business Media

[20] Haidvogel D B and Thomas Zang 1979 The accurate solution of Poisson's equation by expansion in Chebyshev polynomials. *Journal of Computational Physics* 30(2): 167–180

[21] Minkowycz W J, Sparrow E M, Murthy J Y and Abraham J P 2009 *Handbook of numerical heat transfer*. John Wiley & Sons, Inc., Hoboken, NJ

[22] Denison M K and Webb B W 1995 Development and application of an absorptionline blackbody distribution function for CO_2. *International Journal of Heat and Mass Transfer* 38(10): 1813–1821

[23] Pearson J T, Webb B W, Solovjov V P and Jiefu Ma 2014 Efficient representation of the absorption line blackbody distribution function for H_2O, CO_2, and CO at variable temperature, mole fraction, and total pressure. *Journal of Quantitative Spectroscopy and Radiative Transfer*, 138: 82–96

[24] Hottel H C and Sarofim A F 1965 *Radiative transport*. McGraw Hill, New York

[25] Hongmei Zhang and Modest M F 2002 Evaluation of the Planck-mean absorption coefficients from HITRAN and HITEMP databases. *Journal of Quantitative Spectroscopy and Radiative Transfer* 73(6): 649–653

[26] Solovjov V P and Webb B W 2000 SLW modeling of radiative transfer in multicomponent gas mixtures. *Journal of Quantitative Spectroscopy and Radiative Transfer*, 65(4): 655–672